

## نانوخوشه‌های منگنز دی اکسید به عنوان یک نانوجاذب بالقوه برای حذف یون نقره از آب

حسن کریمی\*، بحرعلی نجفی

گروه شیمی، دانشگاه پیام نور، صندوق پستی ۳۶۹۷-۱۹۳۹۵، تهران، ایران  
تاریخ دریافت: ۲۹ اردیبهشت ۱۳۹۴ تاریخ پذیرش: ۸ شهریور ۱۳۹۴

### Manganese Dioxide Nanoclusters As a Potential Nano-Sorbent for The Removal of Silver Ion from Water

Hassan Karami\*, Bahr Ali Najafi

Department of Chemistry, Payame Noor University, 19395-4697, Tehran, I.R. of Iran

Received: 19 May 2015

Accepted: 30 August 2015

#### چکیده

نانوخوشه‌های منگنز دی اکسید نمناک از اکسیداسیون یون‌های منگنز(II) به وسیله محلول آمونیاک پروسولفات تهیه و به عنوان جاذب جدیدی برای یون‌های نقره و حذف آن از محیط‌های آبی استفاده شد. ویژگی‌های ترکیب سنتز شده به وسیله میکروسکوپ الکترونی روبشی (SEM)، (DLS)، EDAX، XRD و BET مشخص شد. تصاویر SEM نشان داد که نانوخوشه‌های منگنز دی اکسید نمناک سنتز شده شامل نانوخوشه‌های جوجه تیغی شکل، با سوزن‌های به قطر ۳۶ nm و طول ۱۰۰۰ nm می‌باشد. از داده‌های XRD معلوم شد که در این روش آلوتروپ  $\gamma$ - $MnO_2$  تشکیل می‌شود. دسته‌ای از آزمایش‌ها نشان داد که نانوخوشه‌های منگنز دی اکسید نمناک دارای ظرفیت جذب  $Ag^+$  می‌باشد. ماکزیمم جذب بوسیله مدل لانگمیر برای یون نقره  $97/81 \text{ mg.g}^{-1}$  برآورد شد. جذب یون نقره بر روی نانوخوشه‌های منگنز دی اکسید نمناک از فرایندهای سرعتی و سینتیکی پیروی می‌کند. عوامل مؤثر در حذف یون نقره از روی نانوخوشه‌های منگنز دی اکسید نمناک به مقدار pH و دمای محلول بستگی دارد. در حضور یون‌های  $Ca^{2+}$ ،  $Na^+$  و  $Mg^{2+}$  با غلظت پایین‌تر از ۲۰۰ ppm تأثیر معنی‌داری برای حذف یون نقره نداشت. یون‌های جذب‌شده به آسانی با حجم کوچکی از یک محلول تی‌اوره و هیدروکلریک اسید شسته شد. سرانجام داده‌های آزمایشات نشان داد که می‌توان از نانوخوشه‌های منگنز دی اکسید نمناک سنتز شده، برای حذف یون نقره از نمونه آب‌های واقعی استفاده کرد.

#### واژه‌های کلیدی

نانوخوشه‌های منگنز دی اکسید آبدار؛ اکسیداسیون شیمیایی؛ نانوجاذب؛ حذف یون نقره.

#### Abstract

Hydrous manganese dioxide nanoclusters are prepared by the oxidation of manganese (II) ions with ammonium persulfate and used as a new sorbent for  $Ag^+$  ion removal from aqueous medium. The synthesized compound is characterized using scanning electron microscopy, dynamic light scattering, energy dispersive analysis of X-rays, X-ray diffraction and BET surface measurements. Scanning electron microscopy images showed that the synthesized Hydrous manganese dioxide nanoclusters include cactus-shaped nanoclusters with uniform needles of average diameter of 36 nm and length of 1000 nm. X-ray diffraction data reveal that  $\gamma$ - $MnO_2$  is formed in this method. Batch experiments are carried out to evaluate the  $Ag^+$  adsorption capacity of Hydrous manganese dioxide nanoclusters. The maximum adsorption capacity estimated by the Langmuir model was  $81.97 \text{ mg g}^{-1}$  for  $Ag^+$ . Silver ion adsorption on Hydrous manganese dioxide nanoclusters is a fast process and the kinetics followed a pseudo-second-order rate equation. The removal efficiency of  $Ag^+$  depends on Hydrous manganese dioxide nanoclusters amount, pH and temperature of the solution. The presences of  $Na^+$ ,  $Ca^{2+}$  and  $Mg^{2+}$  ions in the concentrations lower than 200 ppm have no significant influence on silver ion removal. The adsorbed ions can easily eluted by the small volume of a solution consisting thiourea and hydrochloric acid. Finally, the experimental data show that the synthesized Hydrous manganese dioxide nanoclusters can quantitatively remove silver ions from real water samples.

#### Keywords

Hydrous Manganese Dioxide Nanoclusters; Chemical Oxidation; Nano-Sorbent; Silver Ion Removal.

#### 1. INTRODUCTION

As the worldwide legislative trends are leading to the lowest discharge levels of naturally occurring metal ions in effluents, continuous increase of the

world's need for most of the metal and metal compounds and also the decrease in grade of the available ores make it essential to find suitable methods to process wastewaters containing metal

ions, even at very low concentrations. On the other hands, environmental regulations on the discharge of heavy metal ions and rising demand for clean water with extremely low level of heavy metal ions make it greatly important to develop different efficient methods for heavy metal ions removal from waters. Conventional treatment processes like chemical precipitation, ion exchange, coagulation and flocculation, electrodialysis, flotation and electrochemical removal have significant disadvantages like incomplete removal, high-energy requirements, and production of toxic sludge [1]. Among the above mentioned different methods, adsorption of heavy metal ions on the surface of solid materials is one of the most recommended physicochemical methods commonly used for heavy metal ions removal from water and wastewater. Adsorption is attractive due to its merits of efficiency, cheap and simple operation [2]. The common sorbents include zeolites, clays, biomass, activated carbon and polymeric materials [3] have low adsorption capacities. Therefore, finding of new promising sorbents are interested and very important in research. Adsorption can be carried out based on the utilization of solid sorbents from either organic, inorganic, biological or mineral compounds [4-5].

Nano-sorbents can be one of the promising ways for a novel environmental purification technique because of producing little or no flocculants and having capability of treating large amounts of water and wastewater within a short time. There are only limited researches on the application of nanomaterials without surface modification in the environmental area [6-19].

Among the available sorbents, metal oxide nanoparticles, including iron oxides, manganese oxides, magnesium oxide, aluminum oxide, titanium oxides, and chromium oxides, are classified as the promising sorbents for heavy metals removal from water and wastewater [6-8]. This is related to their large surface areas and high activities caused by the size-quantization effect [9-10]. Recent reports suggest that many metal oxides exhibit very favorable sorption to heavy metals in terms of high capacity and selectivity, which would result in deep removal of toxic metals to meet increasingly strict regulations [11]. Among of nanomaterials, magnetite [12-13], hematite [14] and maghemite [15-17] nanoparticles have been applied to the removal of different heavy metal ions.

Adsorption of trace heavy metals by manganese oxides has been investigated intensively for a long time [18-19]. It has been showed that manganese oxides adsorb trace heavy metals more strongly than most other sorbents. Recent studies indicate

that manganese dioxide is an effective sorbent in the removal of heavy metals from aqueous solution due to its high adsorption capacity and selectivity [20-30]. Apart from its excellent heavy metal uptake capacity, manganese dioxide is also considered to be an economical and easily available sorbent in the environment. Nevertheless, there is no report about the application of manganese dioxide nanostructures for removal of silver ion from water.

Silver ion is one of the precious heavy metal ions that have significant roles in many parts of human life. Silver ion is widely used in the production of photographic film. Moreover, it is a functional raw material in development of mirroring, electroplating, catalyst, antimicrobial materials, batteries and, coinage, medication industries due to its excellent properties such as malleability, ductility, electrical and thermal conductivity, photosensitivity and antimicrobial. Therefore, there are several sources of entry silver ion pollution in water and wastewaters. The contact with soluble silver compounds may create some toxic effects such as liver and kidney damage, irritation of the eyes, skin, respiratory, and intestinal tract, and changes in blood cells [31]. The World Health Organization (WHO) classified soluble silver ions as hazardous substance in water systems and limited its concentration level in drinking waters lower than  $100 \mu\text{g L}^{-1}$  [32]. So, there is a requirement to develop an effective way for the elimination of silver ions from aqueous solutions. A variety of techniques such as ion exchange [33-34], electrolysis [35], membrane separation [36] and biosorption [37] have been used for the remediation of silver ions from different pollution sources. Because of low cost and simplicity, adsorption methods have also been widely used for removal of silver ions. Several new adsorbents, including activated carbon [38], chelating resins [39], polymeric materials [40], micro and nano-sized functional spheres [41-42], colloidal carbon nanospheres [43] have been investigated to eliminate silver ions from aqueous solutions. An adsorbent must be cheap, available and efficient in the removal of silver ions. Therefore, it is interested to look for low-cost sorbents that could replace synthetic ion exchange resins or other expensive materials.

In the previous study, we presented a low temperature hydrothermal method to prepare uniform cactus-shaped hydrous manganese dioxide nanoclusters (HMDNC) [44]. In current study, we used the previous reported method to synthesize HMDNC. The synthesized HMDNC were additionally characterized (with respect to the previous report) and applied as nano-sorbents for the removal of silver ions from water. The

experimental conditions of adsorption of silver ions on the surface of the synthesized HMDNC were evaluated, and the applicability of HMDNC in silver ions removal from water was evaluated in view of the adsorption kinetic and capacity.

## 2. EXPERIMENTAL

### 2.1. Materials Reagents

All chemicals were of analytical grade and used without further purification. All solutions were prepared with double distilled water. Stock solutions of manganese sulfate (0.8 M) and ammonium persulfate (0.7 M) in sulfuric acid (0.8 M) were prepared freshly. The adsorption experiments were conducted using water spiked with  $\text{Ag}^+$  ions. The stock solutions containing 50 ppm of silver ions were prepared by dissolving appropriate amounts of  $\text{AgNO}_3$ .

### 2.2. Instrumental

The morphology and the particles sizes of the manganese dioxide samples were studied by a LEO scanning electron microscopy (1455 VP model, England). A Philips X'Pert diffractometer with Cu ( $K\alpha$ ) radiation ( $\lambda = 0.15418$  nm) was used to study the phase composition and the particles sizes of manganese dioxide samples. The temperature of the synthesis solutions was kept constant by a water bath (Pars Azma Co., Iran). Surface area, pore size and pore volume were analyzed by Brunauer–Emmett–Teller (BET) (model no. AS1C-9) surface area analyzer (Quantachrome Instrument Corp.). Nitrogen adsorption data were taken at five relative pressures at 77 K to calculate the surface area by BET theory. Dynamic light scattering measurements to determine size distribution were performed by ZEN 3600 (Molvern Co.).

Each measurement was performed in an aqueous solution with a constant ionic strength of 0.01M  $\text{KNO}_3$ , pH was adjusted by adding drops of  $\text{NaOH}$  or  $\text{HNO}_3$  solution. The metal ions concentration were determined by a Sens AA model flame atomic absorption spectroscopy (FAAS) from GBC Co. (Australia). For confirming the obtained data via the proposed method, Nex ION 300D ICP-MS was used to analyze the real samples.

### 2.3. Procedure

#### 2.3.1. Synthesis procedures

The synthesis procedure was exactly similar with the previous report [44].  $\gamma\text{-MnO}_2$  was synthesized by low temperature hydrothermal method as following. Reagent grade manganese sulfate ( $\text{MnSO}_4$ ) and ammonium persulfate ( $(\text{NH}_4)_2\text{S}_2\text{O}_8$ ) solutions were used as the precursors. The equal volumes of  $\text{MnSO}_4$  (0.8 M) and  $(\text{NH}_4)_2\text{S}_2\text{O}_8$  (0.7

M) solutions containing 0.8 M sulfuric acid were heated to reach the desired temperature (80 °C). The obtained solutions were mixed in constant temperature to form hydrous  $\text{MnO}_2$  during 1 h. After reaction completion, the precipitate was separated from the solution, washed with water and ethanol and dried at room temperature.

#### 2.3.2. Adsorption experiments

50 mg HMDNC sorbent was added into the 50 ml of 10 ppm silver ion solution in adjusted pH and room temperature (25 °C). After a period of time, the sorbent was separated from the solutions using a cellulose acetate membrane filter, and the final metal ions concentrations (non adsorbed ions) were determined by the flame atomic absorption spectroscopy (FAAS).

The effects of all efficient parameters such as pH, retention temperature, sorbent weight,  $\text{Ag}^+$  concentration, sample volume, mixing time of nanosorbent with sample solution (equilibrium time), and eluent type and concentration were fully investigated and optimized by the "one at a time" method.

The adsorbed amount of metal ions onto the HMDNC sorbent was calculated according to the following equation (Eq. 1):

$$\text{Removal efficiency(\%)} = \frac{C_i - C_f}{C_i} \times 100 \quad (1)$$

Where,  $C_i$  (ppm) and  $C_f$  (ppm) are initial concentrations and the concentration of heavy metal ions after adsorption, respectively. The equilibrium adsorption capacity,  $q_e$  ( $\text{mg g}^{-1}$ ) of heavy metal ions was calculated using the mass balance equation (Eq. 2):

$$q_e = \frac{(C_i - C_e)V}{m} \quad (2)$$

Where,  $C_i$  (ppm) and  $C_e$  (ppm) are initial concentration and equilibrium concentration of metal ions, respectively; V (ml) is the sample volume, m (mg) is the mass of HMDNC nanosorbent.

#### 2.3.3. Effect of equilibration time

The effect of contact time on metal ion adsorption was studied in different time intervals ranging from 1 min to 120 min with the initial metal ions concentration of 10 ppm. After completing of the treatment, conical flasks were taken out and the HMDNC sorbents were separated followed by the determination of the residual metal ions concentration.

#### 2.3.4. Effect of initial metal ions concentration

Adsorption isotherms were obtained by equilibrating HMDNC sorbent with metal ion

solutions of different initial concentrations of 1–100 ppm for 30 min. After separation, the final concentrations of metal ions in the solutions were measured.

### 2.3.5. Effect of pH

Adsorption behaviors of 10 ppm  $\text{Ag}^+$  and 30 min equilibration time were studied as a function of pH. The initial pH values were adjusted from 1 to 8, using 0.1 M  $\text{HNO}_3$  or NaOH solution. After contacting for 30 min, the suspensions were separated and the residual metal ions concentrations were analyzed.

### 2.3.6. Desorption studies

After optimizing of adsorption experiments, the elution step is studied. Some solvents such as  $\text{HNO}_3$ , HCl,  $\text{HNO}_3$ +HCl and HCl+thiourea (with different concentrations) were examined as eluent for desorption of the adsorbed ions in 1 ml volume.

### 2.3.7. Application in real samples

The presented method was used to determine the silver contents of some real water samples which were sampled from Tekab industrial zoon (Iran). To determine the  $\text{Ag}^+$  concentration in real waters, 50 mg HMDNC powder was added to 500 ml real water followed by mixing in 500 rpm for 1 h. The sorbent nanoparticles were filtered and the adsorbed ions eluted by 1 ml HCl + thiourea as eluent solution. The silver ion concentration in the eluted solution was determined. The desorbed amount of silver ions was calculated according to the following equation (Eq. 3):

$$\text{Sample concentration (ppb)} = \frac{C_f \times V_f}{V_i} \times 1000 \quad (3)$$

Where,  $C_i$  (ppb) and  $V_i$  (ml) are initial concentration and initial volume of real sample.  $C_f$  (ppm) and  $V_f$  are the final concentration and final volume of the eluted solution, respectively.

## 3. RESULTS AND DISCUSSION

### 3.1. Properties of prepared HMDNC

To insure about the similarity of the synthesized HMDNC with the previous report [44], the morphology, particles sizes and the composition of the sample were again characterized by SEM, XRD, and additionally by BET and DLS. Fig. 1 shows the SEM images of the synthesized sample. As it is obvious in Fig. 1, the morphology and the particles sizes of the sample are the same as in the Ref. [44]. The SEM images illustrated that the synthesized HMDNC were cactus-shaped nanoclusters including needles with average

diameter of 36 nm and average length of 1000 nm.

The specific surface area of the prepared HMDNC was determined by the nitrogen adsorption analysis (BET method). Sample was degassed at 100 °C for 1 h under vacuum prior to analysis.

The nitrogen adsorption- desorption isotherms on the surface of the synthesized HMDNC are showed in Fig. 2. By using BET method, the surface area of HMDNC sorbent was found to be  $210.4 \text{ m}^2 \text{ g}^{-1}$ . BET results showed that the synthesized HMDNC has bigger surface area with respect to the previous reported manganese dioxide nanoparticles [45-47]. Such high surface area can be considered to be efficient through the adsorption process. In addition, the HMDNC sorbent posses high pore volume of  $0.21 \text{ cm}^3 \text{ g}^{-1}$  and an adsorption average pore width of 65.1 nm.

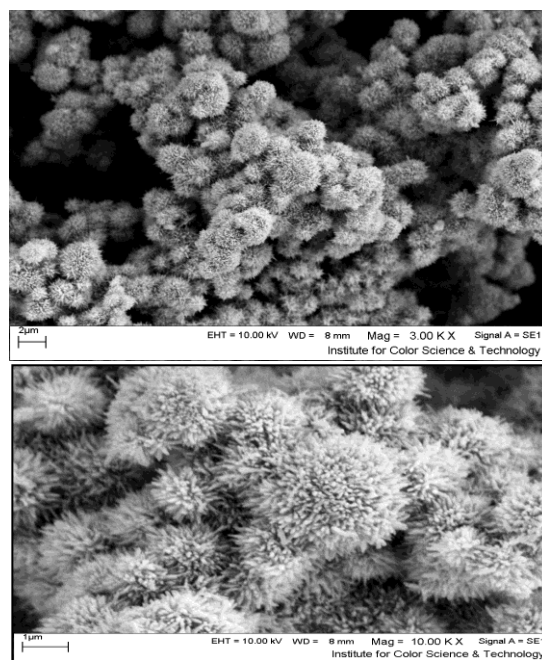


Fig. 1. SEM images of the synthesized HMDNC in two magnifications of 3000 (a) and 10000 (b).

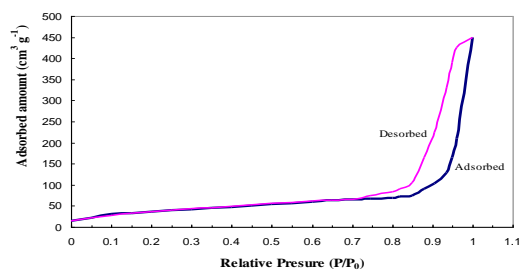
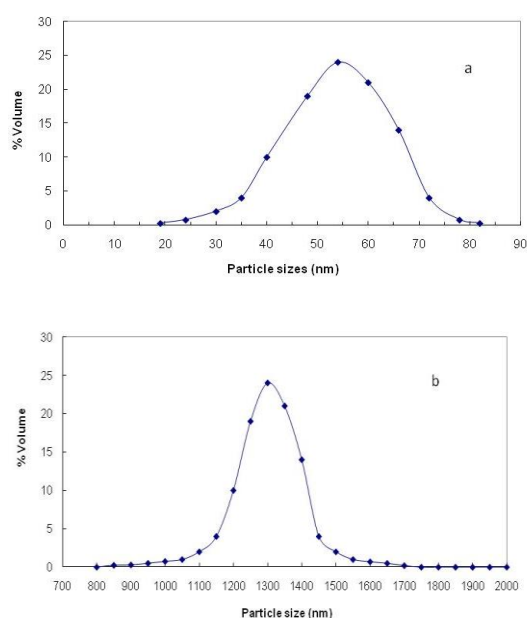


Fig. 2. BET analysis of the synthesized HMDNC based on the adsorption/desorption of  $\text{N}_2$  gas.

The position of the XRD peaks show good agreement with those of  $\gamma\text{-MnO}_2$  as Ref [44].

Therefore, the XRD patterns are not shown in this paper. The synthesized HMDNC was studied by FT-IR spectroscopy. The FT-IR spectrum showed that the synthesized sample includes many hydroxyl groups in the surface of particles (a wide and big peak in  $3400\text{ cm}^{-1}$  is related to hydroxyl functional group). Therefore, the synthesized sample is in hydrous form. To determine the distribution range of particles sizes, the HMDNC sample was analyzed by DLS. Fig. 3 shows the DLS diagram for the HMDNC sample. As it can be seen in Fig. 3, there are two zones for size distribution. First zone starts from 20 to 80 nm (average: 55nm) which it is related to the diameter of needles. Second zone is related to the diameter of the cactus shape particles which starts from 1000 to 1500 nm (average: 1300 nm).



**Fig. 3.** Size distribution diagram for the synthesized HMDNC obtained by dynamic light scattering technique (DLS); in the range of 0 to 90 nm (a) and in the range of 700 to 2000 nm (b).

### 3.2. Adsorption study

#### 3.2.1. Adsorption kinetics

In kinetic study, 50 mg HMDNC was added into 50 ml solutions of  $\text{Ag}^+$  10.0, 20.0, 30.0 and 40.0 ppm, respectively. The pH was kept at  $5.0 \pm 0.1$  and the mixture was mixed at 500 rpm. The samples were taken at different interval times, filtered through a  $0.45\ \mu\text{m}$  membrane and analyzed for the  $\text{Ag}^+$  concentrations by an atomic absorption spectrophotometer. The results of adsorption investigations carried out as a function of contact time (mixing time), were presented in Fig. 4. Based on the experimental data the contact time of 30 min was chosen for further

experiments. As Fig. 4a shows, the removal of  $\text{Ag}^+$  ions by the HMDNC sorbent with efficiencies more than 95% took place during 20 min, this time is faster than those of the previous reports for  $\text{Ag}^+$ , 50 min [48,49] and 120 min [50]. For kinetic studies, the pseudo first-order and pseudo second-order models were investigated and the experimental data showed that the pseudo second-order model is more consistent with the data. The pseudo-second order equation assumes that the adsorption process involves chemisorption mechanism and the rate of site occupation is proportional to the square of the number of unoccupied sites [51]. If the rate of adsorption is a second order mechanism, the pseudo-second order chemisorption kinetic rate equation will be as following (Eq. 4):

$$\frac{d_p}{d_t} = k_2(q_e - q_t)^2 \quad (4)$$

where  $k_2$  is pseudo-second order rate constant ( $\text{g mg}^{-1} \text{min}^{-1}$ ). After integrating at boundary conditions ( $t = 0$  and  $q = 0$ ), the following equation will be obtained:

$$\frac{t}{q_t} = \frac{1}{K_2 q_e^2} + \frac{t}{q_e} \quad (5)$$

where  $k_2$  ( $\text{g mg}^{-1} \text{min}^{-1}$ ) is the rate constant.  $q_e$  ( $\text{mg g}^{-1}$ ) and  $q_t$  ( $\text{mg g}^{-1}$ ) are the amounts of metal ions adsorbed at equilibrium time and at any time ( $t$ ), respectively. In order to determine the rate constant of pseudo-second order model, the adsorption data during 50 min was used for 40 ppm  $\text{Ag}^+$  solution. The linear plots of  $t/q_t$  vs.  $t$  obtained for the adsorption of  $\text{Ag}^+$  onto HMDNC sorbent at different solution temperatures were shown in Fig. 4b. The  $R^2$  values and the pseudo-second-order model parameters were shown in Table 1.

**Table 1.** Kinetic parameters obtained from pseudo-second-order model applied for the adsorption of  $\text{Ag}^+$  onto MDNC.

Temperature ( $^{\circ}\text{C}$ )	$K_2$ ( $\text{g mg}^{-1} \text{min}^{-1}$ )	$q_e$ ( $\text{mg g}^{-1}$ )	$R^2$
10	0.373	1.242	0.999
20	0.455	0.934	0.999
30	0.600	0.779	0.999
40	0.500	0.688	0.999

#### 3.2.2. Isothermal Studies

Silver ion removal performance of HMDNC was investigated as a function of the initial silver ion concentration (from 1 ppm to 100 ppm) at a pH value of 4.0. In this study, the adsorption time was fixed at 30 min because the adsorption of  $\text{Ag}^+$  ions onto the HMDNC sufficiently reached an equilibrium state for 30 min based on the data of Fig. 4a. Fig. 5 shows the effect of initial ion

concentration and initial sample volume on the removal efficiency. As it can be seen in Fig. 5a, the removal of  $\text{Ag}^+$  ions at concentration of 80 ppm and lower is complete. By increasing metal ion concentration from 80 to 100 ppm, removal efficiency decreases. This concept can be related to this fact that the surface sites of HMDNC are occupied at higher concentration. With respect to the 50 ml sample volume, the adsorption capacity is estimated  $80 \text{ mg (Ag) g}^{-1}$  (HMDNC).

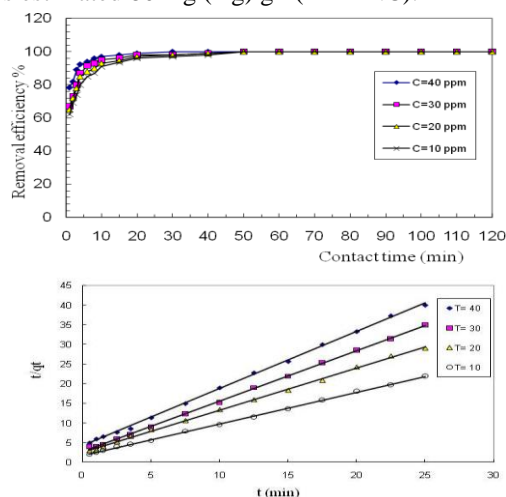


**Fig. 4.** (a) Effect of contact time on the silver ions removal efficiency at different initial concentrations of  $\text{Ag}^+$  and (b) Linearized pseudo-second order kinetic curves for the silver ion adsorption on the surface of HMDNC at  $\text{pH}=5.0$  and four temperatures (10, 20, 30 and  $40^\circ\text{C}$ ).

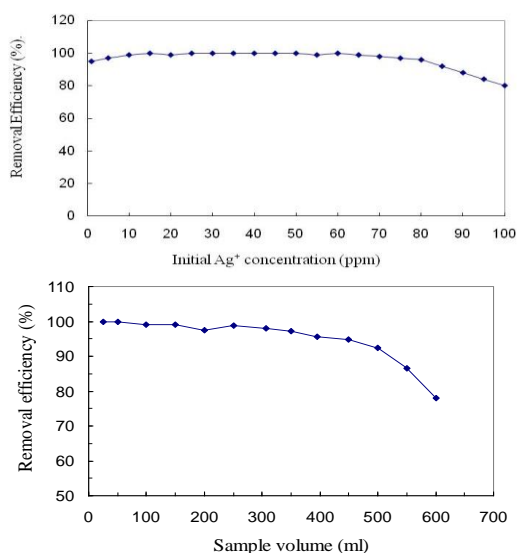


**Fig. 5.** Effects of initial concentration of silver ion (a) and initial volume of silver ion solution (b) on the removal efficiency.

To obtain Fig. 5b, 2.50 mg silver ion was dissolved in different volumes. As Fig. 5b shows that the silver ion removal at sample volumes of

500 ml and lower is more than 95%. By increasing the sample volume from 500 to 600 ml, the removal efficiency decreases. Increasing sample volume causes to decrease the equilibrium concentration of metal ions in the solution so that the equilibrium removal will be decreased. When the same number of metal ions is distributed in two different volumes, the distance between ions in large volume is more so, the ion removal in small volume of solution will be easier. To determine the adsorption capacity of HMDNC towards silver ions, adsorption studies over a large initial concentration range from 80 to 180 ppm were carried out. These initial concentrations make silver ion concentrations in the range of 0 to 100 ppm in the equilibrium state. The maximum adsorption capacity of the HMDNC sorbent for silver ions was evaluated using the adsorption isotherms. Langmuir and Freundlich isotherm models were applied for isotherm adsorption analysis of the obtained adsorption data. In the Langmuir model, it is assumed that all the adsorption sites of the sorbent have an identical binding energy and each site binds to only a single ion [52]. The linearized Langmuir isotherm is given as:

$$\frac{C_e}{q_e} = \frac{1}{bq_m} + \frac{C_e}{q_m} \quad (6)$$

Where,  $q_e$  is the equilibrium adsorption capacity of sorbent for metal ions in  $\text{mg g}^{-1}$ ,  $C_e$  is the equilibrium concentration of metal ions in ppm,  $q_m$  is the maximum amount of metal ions adsorbed in  $\text{mg g}^{-1}$ , and  $b$  is the constant that refers to the bonding energy of adsorption process in  $\text{L mg}^{-1}$ . The constants  $b$  and  $q_m$  can be determined from the intercept and slope of the linear plot  $C_e/q_e$  versus  $C_e$ . On the contrary, the Freundlich model is based on a reversible heterogeneous adsorption; heterogeneity of binding energies of adsorption sites [39]. The linearized Freundlich isotherm can be given as following:

$$\log q_e = \log k_f + \frac{1}{n} \log C_e \quad (7)$$

where  $q_e$  is the equilibrium adsorption capacity of the sorbent in  $\text{mg g}^{-1}$ ,  $C_e$  is the equilibrium concentration of silver ions in ppm,  $K_f$  is the constant related to the adsorption capacity of the sorbent in ppm, and  $n$  is the constant related to the adsorption intensity. The constants  $n$  and  $K_f$  can be determined from the slope and intercept of the linear plot  $\log q_e$  versus  $\log C_e$ . The quantitative relationship between initial silver ion concentration and the adsorption capacity was analyzed with two different isotherm models. The Langmuir isotherm was better fit with the experimental data. Therefore, only Langmuir isotherm was shown in Fig. 6.

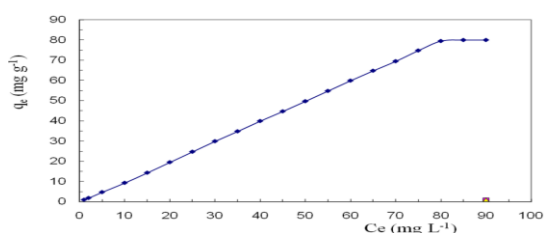


**Fig. 6.** Linearized Langmuir isotherm for the adsorption of silver ions on the HMDNC surface at pH=5.0 and T=25 °C.

The calculated correlation coefficients ( $b$  and  $q_m$ ) and linear regression coefficient ( $R^2$ ) values for Langmuir model are  $-0.37$  ( $L\ mg^{-1}$ ),  $81.97$  ( $mg\ g^{-1}$ ) and  $0.99$ , respectively. Based on the Langmuir model, adsorption capacity of  $Ag^+$  ions by HMDNC was calculated  $81.97\ mg\ g^{-1}$ . The capacity was determined for single-solute system. The adsorption efficiency of HMDNC for  $Ag^+$  in a multi-solutes system consisting  $Fe^{2+}$ ,  $Pb^{2+}$ ,  $Zn^{2+}$ ,  $Ni^{2+}$ ,  $Cd^{2+}$  and  $Cu^{2+}$  with the 200 ppm initial concentrations were determined. The contact time and filtering and concentration determination were the same as single-solute system. Analytical concentrations of the silver ions in the filtrate solution ( $C_f$ ) were used to calculate the adsorption values based on the following equation:

$$q_{mix} = \frac{1000(C_i - C_f)}{50} \quad (8)$$

Where,  $q_{mix}$  ( $mg\ g^{-1}$ ),  $C_i$  (ppm) and  $C_f$  (ppm) are the adsorption value, initial concentration and final concentration of the proposed ion in the multi-solute system, respectively. The adsorption value  $Ag^+$  ions in the presence of  $Fe^{2+}$ ,  $Pb^{2+}$ ,  $Zn^{2+}$ ,  $Ni^{2+}$ ,  $Cd^{2+}$  and  $Cu^{2+}$  in the multi-solute system were calculated as  $67\ mg\ g^{-1}$ . Comparing of the capacity values in multi-solute system with the calculated adsorption capacities in single-solute system shows that the presence of several different ions in the initial solution decrease the maximum adsorption of silver ion from  $81.97$  to  $67\ mg\ g^{-1}$ .

### 3.2.3. Effect of pH

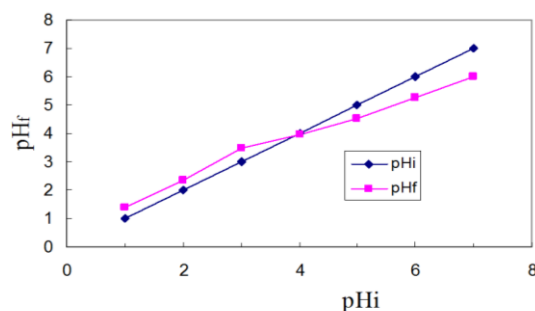
To determine the point of zero-charge (PZC) for HMDNC, seven samples with pH of 2, 3, 4, 5, 6, 7 and 8 were prepared by adding  $HNO_3$  or  $NaOH$  solutions. To each solution, 100 mg HMDNC was added and mixed for 30 min at 500 rpm. The final pH is determined for each sample. Fig. 6a shows the results of these studies. The data presented in Fig. 7a shows that the surface of HMDNC particles are charge free at  $pH = 4$ . At higher pH, the surface of HMDNC particles include negative charge and at lower pH, they have positive charge.

The influence of sample pH on the silver ion removal is experimentally studied. The silver ion removal in the above mentioned pH was

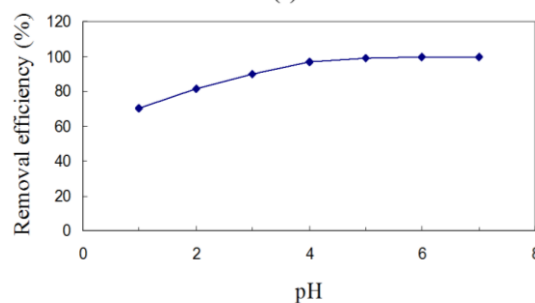
examined. Fig. 7b shows that the silver ion removal at pH range of 4-7 is complete. Based on the zero-charge pH studies, silver ions can be taken by negatively charged sites of HMDNC. The removal experiments should be done at pH lower than 6 because, silver hydroxide precipitation can be formed at alkaline pH.

### 3.2.4. Effect of temperature on the metal ions removal

Based on the previous reports about metal ions removal by metal oxides, ion removal efficiency depends strongly on the solution temperature [53-54]. Therefore, removal of silver ions from aqueous solutions was done at five temperatures of 10, 20, 30, 40 and 50 °C. Fig. 8 shows that how temperature changes the silver ion removal efficiency.



(a)



(b)

**Fig. 7.** Determination of PZC for the HMDNC (a) and relationship between the initial pH values and the efficiency of silver ion removal (b).

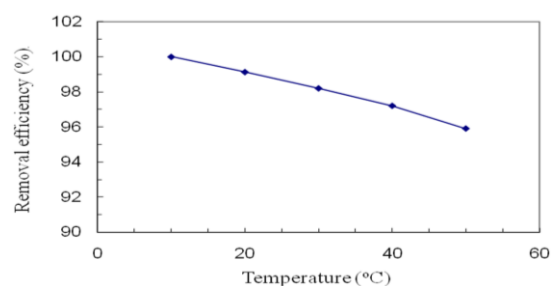


**Fig. 8.** Effect of solution temperature on the silver ion removal efficiency by HMDNC sorbent at pH=5.0 and T=25 °C, sample volume 50 ml and HMDNC weight 50 mg.

Adsorption of silver ions on the surface of HMDNC was slightly decreased by elevation of solution temperature, which implied the exothermic nature of the  $\text{Ag}^+$  ion sorption on HMDNC particles. This fact can be evaluated by the thermodynamic parameters, such as the change of Gibbs free energy of sorption ( $\Delta G$ ), the heat of sorption ( $\Delta H$ ), and the standard entropy change ( $\Delta S$ ) were calculated according to the van't Hoff equation [55]. The calculated thermodynamic parameters were summarized in Table 2. The negative  $\Delta H$  and  $\Delta G$  shows the process was essentially an exothermic and spontaneous one.

**Table 2.** Thermodynamic parameters of  $\text{Ag}^+$  adsorption onto HMDNC surface.

Temperature (°C)	$\Delta G$ (kJ mol <sup>-1</sup> )	$\Delta H$ (kJ mol <sup>-1</sup> )	$\Delta S$ (J mol <sup>-1</sup> K <sup>-1</sup> )
10	-22.11	-11.64	49.14
20	-25.87		58.83
30	-27.17		64.75
40	-29.08		67.31

### 3.2.5. Removal efficiency in the presence of other ions

Concentrations of group IA and IIA metal ions in major real samples are higher than heavy metal ions. Therefore, we investigate the effect of potassium (as example of IA metal ions), calcium (as example of IIA metal ions) and some heavy metal ions such as  $\text{Fe}^{2+}$ ,  $\text{Pb}^{2+}$ ,  $\text{Zn}^{2+}$ ,  $\text{Ni}^{2+}$ ,  $\text{Cd}^{2+}$  and  $\text{Cu}^{2+}$  with different concentrations (Fig. 9).

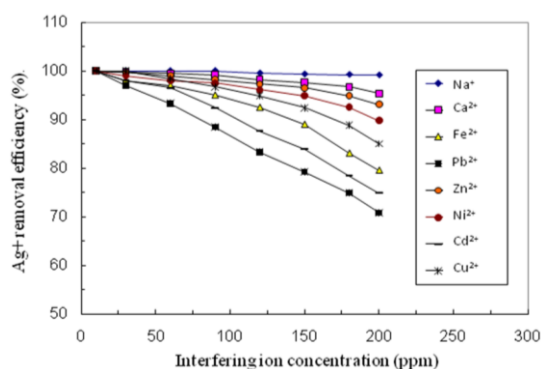


**Fig. 9.** Effects of some interfering ions on the silver ion removal by HMDNC.

As it can be seen in Fig. 9, the silver ion removal in the presence of sodium ions with any concentration is complete. The other studied ions can slightly affect on the silver ion removal efficiency. Therefore, silver ions can selectively removed by HMDNC in the presence of different ions. Based on the obtained data, the following order shows the interfering amounts of the investigated ions on the  $\text{Ag}^+$  removal:  $\text{Ag}^+ \gg \text{Pb}^{2+} > \text{Cd}^{2+} > \text{Fe}^{2+} > \text{Cu}^{2+} > \text{Ni}^{2+} > \text{Zn}^{2+} > \text{Ca}^{2+}$

The concentrations of not adsorbed sodium and calcium ions were determined by ICP- atomic spectroscopy. The analytical results showed that the sodium and calcium ions concentrations on the filtrate solution were 199 and 195 ppm, respectively. The adsorption percentages for sodium and calcium ions were 0.5 % and 2.5 %, respectively. In a separate experiment, a 50 mg HMDNC was added to a 50 ml solution consisting 50 ppm sodium and 50 ppm calcium. The removal efficiencies of sodium and calcium ions were calculated as those of silver ions. The experimental data showed that the removal efficiencies for sodium and calcium in diluted solution were 0.2% and 1.5%, respectively. The obtained results showed that the IA and IIA metal ions cannot considerably adsorbed on the HMDNC and also they are not effective inhibitors for adsorption of silver ions on the surface of HMDNC. Therefore, HMDNC can be used as effective sorbent for silver ions in all water samples which includes alkaline and earth alkaline metal ions.

### 3.3. Elution of the adsorbed silver ions

The elution power of some ordinary solvents such as Ammonia solution, HCl,  $\text{HNO}_3$  and  $\text{HCl} + \text{HNO}_3$  solutions, and some organic solvents such as ethanol, chloroform, acetonitrile, dimethyl formamide (DMF) and acetone were examined. Any of the examined solvents could not quantitatively make desorption the adsorbed silver ions. Thiourea can be used as a ligand to form a complex with heavy metal ions such as silver ions. Therefore, thiourea as complex agent was added to HCl solution. The mixed solutions including 3 M HCl and different concentration of thiourea were examined. Fig. 10 shows the effect of thiourea concentration on the silver ion recovery. As it can be seen in Fig. 10, HCl solution consisting at least 6 %wt thiourea can completely recover the silver ions.

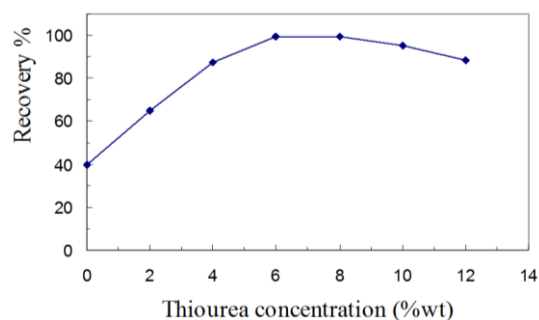


**Fig. 10.** Effect of thiourea concentration on the recovery of adsorbed silver ions.

Experimental results showed that the eluent consisting more concentrations of thiourea than 6

%wt can slightly dissolve the HMDNC so that, the recovery decreases and the HMDNC sorbent can be used only a few times. To calculate reproducibility of adsorption/elution processes, 50 mg HMDNC was used to adsorb 50 ppm silver ion from 50 ml solution. After collecting the HMDNC particles, these nanomaterials were washed by distilled water to remove the trapped solvent molecules for three times. Finally, the adsorbed ions were recovered by HCl + thiourea. In second time, the washed nanomaterials were again used to remove silver ions from another 50 ml solution. These experiments (adsorption/elution/washing) were repeated for 5 times. The obtained results were summarized in Table 3. As it can be seen in this table, the capacity of HMDNC sorbent decreases when the sorption/desorption cycles increases so that the proposed sorbent is not reusable more than 3 times because, a part of nano- sorbent is dissolved in HCl solvent in each elution.

**Table 3.** Effects of adsorption/desorption cycles of silver ions on the removal efficiency.

Cycle No.	1	2	3	4	5
Removal %	99	95	90	80	70

#### 3.4. Application in real samples

To evaluate the accuracy of the presented method in real samples, four real waters were collected from four industrial zones in Iran. For each sample, 50 mg HMDNC was added to 500 ml unspiked sample. The sample was mixed for 30 min at 500 rpm mixing rate. The HMDNC particles were filtered and washed with distilled water. Finally, the adsorbed ions were eluted by 3 ml solvent (3 M HCl + 8 %wt thiourea). The silver ion concentration was determined by atomic absorption spectroscopy. Based on the silver ion concentration in the eluted solution, its concentration in initial sample was calculated. Comprehensive analysis of all samples was done by ICP-Mass Spectroscopy (ICP-MS). Table 4 summarizes the obtained results. The experimental data shows that the presented method can be used as a powerful analytical technique to determine the silver ion concentration in real waters.

**Table 4.** Comprehensive analysis of four real water samples from four zones in West Azarbayegan state by the proposed method and ICP-MS (replicates = 3).

Zoon	Aghdarreh	Tekab	Takhte Soleyman	Zareh Shooran
Proposed method	4.48±0.08	1.4±0.02	1.02±0.02	9.30±0.20
ICP-MS	4.40±0.20	ND*	ND	9.00±0.20

\*ND = Not detectable

## CONCLUSIONS

Crystallized hydrous manganese dioxide nanoclusters (HMDNC) in cactus shape can be synthesized by the low temperature hydrothermal method. HMDNC is a potential and fast sorbent for the removal of silver ions from polluted water. Silver ion removal by HMDNC is depends strongly on pH and solution temperature. Basen on the experimental data, silver ion adsorption on the HMDNC can be explained by the Langmuir isotherm. The adsorbed ions on the HMDNC surface can be eluted by acidic solution of thiourea. Therefore, HMDNC can reused for the silver ion removal for several times.

## ACKNOWLEDGEMENT

We gratefully acknowledge the support of this work by Abhar Payame Noor University Research Council.

## REFERENCES

- [1] F. Fu and Q. Wang, Removal of heavy metal ions from wastewaters: a review, *J. Environ. Manag.* 92 (2011) 407–418.
- [2] G. Crini, Recent developments in polysaccharide-based materials used as sorbents in wastewater treatment, *Prog. Polym. Sci.* 30 (2005) 38–70.
- [3] G. Crini, Non-conventional low-cost sorbents for dye removal: a review, *Bioresour. Technol.* 97 (2006) 1061–1085.
- [4] V. Camel, Solid phase extraction of trace elements, *Spectrochim. Acta Part B* 58 (2003) 1177–1233.
- [5] P.K. Jal, S. Patel and B.K. Mishra, Chemical modification of silica surface by immobilization of functional groups for extractive concentration of metal ions, *Talanta* 62 (2004) 1005–1028.
- [6] J.E. Vanbenschoten, B.E. Reed, M.R. Matsumoto and P.J. McGarvey, Metal removal by soil washing for an iron-oxide coated sandy soil, *Water Environ. Res.* 66 (1994) 168–174.
- [7] J.A. Coston, C.C. Fuller and J.A. Davis, Pb<sup>2+</sup> and Zn<sup>2+</sup> adsorption by a natural aluminum-bearing and iron-bearing surface coating on an aquifer sand, *Geochim. Cosmochim. Acta* 59 (1995) 3535–3547.
- [8] A. Agrawal and K.K. Sahu, Kinetic and isotherm studies of cadmium adsorption on manganese nodule residue, *J. Hazard. Mater.* 137 (2006) 915–924.
- [9] A. Henglein, Small-particle research – physicochemical properties of extremely small colloidal metal and semiconductor particles, *Chem. Rev.* 89 (1989) 1861–1873.
- [10] M.A. El-Sayed, Some interesting properties of metals confined in time and nanometer

- space of different shapes, *Acc. Chem. Res.* 34 (2001) 257–264.
- [11] E.A. Deliyanni, E.N. Peleka and K.A. Matis, Modeling the sorption of metal ions from aqueous solution by iron-based sorbents, *J. Hazard. Mater.* 172 (2009) 550–558.
- [12] J. Hu, M.C. Lo and G.H. Chen, Removal of Cr(VI) by magnetite nanoparticles, *Water Sci. Technol.* 50 (2004) 139–146.
- [13] H. Karami, Heavy metal removal from water by magnetite nanorods, *Chem. Eng. J.* 219 (2013) 209–216.
- [14] M. Sadeghi, H. Karami, P. Sarabadani and M. Mirzayee, Separation of  $^{109}\text{Cd}$  from silver target by nanohematite, *Radiochim. Acta* 97 (2009) 733–738.
- [15] M. Sadeghi, P. Sarabadani and H. Karami, Synthesis of maghemite nano-particles and its application as radionuclidic adsorbant to purify  $^{109}\text{Cd}$  radionuclide, *J. Radioanal. Nucl. Chem.* 283 (2010) 297–303.
- [16] A. Roy and J. Bhattacharya, Removal of Cu(II), Zn(II) and Pb(II) from water using microwave-assisted synthesized maghemite nanotubes, *Chem. Eng. J.* 211–212 (2012) 493–500.
- [17] J. Hu, G. Chen and I.M.C. Lo, Removal and recovery of Cr (VI) from wastewater by maghemite nanoparticles, *Water Res.* 39 (2005) 4528–4536.
- [18] H.S. Posselt, F.J. Anderson and W.J. Walter, Cation sorption on colloidal hydrous manganese dioxide, *Environ. Sci. Technol.* 2 (1968) 1087–1093.
- [19] B. B. Johnson, Effect of pH, temperature, and concentration on the adsorption of cadmium on goethite, *Environ. Sci. Technol.* 24 (1990) 112–118.
- [20] S.S. Tripathy, J.L. Bersillon and K. Gopal, Adsorption of  $\text{Cd}^{2+}$  on hydrous manganese dioxide from aqueous solutions, *Desalination* 194 (2006) 11–21.
- [21] W. Zou, R. Han, Z. Chen, J. Zhang and J. Shi, Kinetic study of adsorption of Cu(II) and Pb(II) from aqueous solutions using manganese oxide coated zeolite in batch mode, *Colloids Surf. A* 279 (2006) 238–246.
- [22] M. I. Zaman, S. Mustafa, S. Khan and B. Xing, Effect of phosphate complexation on  $\text{Cd}^{2+}$  sorption by manganese dioxide ( $\gamma\text{-MnO}_2$ ), *J. Colloid Interface Sci.* 330 (2009) 9–19.
- [23] Q. Su, B. Pan, S. Wan, W. Zhang and L. Lv, Use of hydrous manganese dioxide as a potential sorbent for selective removal of lead, cadmium, and zinc ions from water, *J. Colloid Interface Sci.* 349 (2010) 607–612.
- [24] S. Wan, X. Zhao, L. Lv, Q. Su, H. Gu, B. Pan, W. Zhang, Z. Lin and J. Luan, Selective adsorption of Cd(II) and Zn(II) ions by nano-hydrous manganese dioxide (HMO)-encapsulated cation exchanger, *Ind. Eng. Chem. Res.* 49 (2010) 7574–7579.
- [25] K. P. Lisha, S. M. Maliyekkal and T. Pradeep, Manganese dioxide nanowhiskers: a potential sorbent for the removal of Hg(II) from water, *Chem. Eng. J.* 160 (2010) 432–439.
- [26] M.L. Crimi and R.L. Siegrist, Association of cadmium with  $\text{MnO}_2$  particles generated during permanganate oxidation, *Water Res.* 38 (2004) 887–894.
- [27] L. Zhang, J. Ma and M. Yu, The microtopography of manganese dioxide formed in situ and its adsorptive properties for organic micropollutants, *Solid State Sci.* 10 (2008) 148–153.
- [28] R. Liu, H. Liu, Z. Qiang, J. Qu, G. Li and D. Wang, Effects of calcium ions on surface characteristics and adsorptive properties of hydrous manganese dioxide, *J. Colloid Interface Sci.* 331 (2009) 275–280.
- [29] M. Xu, H. Wang, D. Lei, D. Qu, Y. Zhai and Y. Wang, Removal of Pb(II) from aqueous solution by hydrous manganese dioxide: Adsorption behavior and mechanism, *J. Environ. Sci.* 25 (2013) 479–486.
- [30] Q. Su, B. Pan, B. Pan, Q. Zhang, W. Zhang, L. Lv, X. Wang, J. Wu and Q. Zhang, Fabrication of polymer-supported nanosized hydrous manganese dioxide (HMO) for enhanced lead removal from waters, *Sci. Total Environ.* 407 (2009) 5471–5477.
- [31] H.Y. Huo, H.J. Su and T.W. Tan, *Chem. Eng. J.* 150 (2009) 139–144.
- [32] M. Hosoba, K. Oshita, R.K. Katarina, T. Takayanagi, M. Oshima and S. Motomizu, *Anal. Chim. Acta* 639 (2009) 51–56.
- [33] N. Lihareva, L. Dimova, O. Petrov and Y. Tzvetanova, *Micropor. Mesopor. Mater.* 130 (2010) 32–37.
- [34] M.J. Manos, C.D. Malliakas and M.G. Kanatzidis, *Eur. J.* 13 (2007) 51–58.
- [35] B. Pollet, J.P. Lorimer, S.S. Phull and J.Y. Hihn, *Ultrason. Sonochem.* 7 (2000) 69–76.
- [36] A.R. Ladhe, P. Frailie, D. Hua, M. Darsillo, D. Bhattacharya, *J. Membr. Sci.* 326 (2009) 460–471.
- [37] Z. Lin, C. Zhou, J. Wu, J. Zhou and L. Wang, *Spectrochim. Acta A* 61 (2005) 1195–1200.
- [38] P. Vassileva, P. Tzvetkova, L. Lakov and O. Peshev, *J. Porous Mater.* 15 (2008) 593–599.

- [39] H. Yirikoglu and M. Gulfen, *Sep. Sci. Technol.* 43 (2008) 376-388.
- [40] M.A.A. El-Ghaffar, M.H. Mohamed and K.Z. Elwakeel, *Chem. Eng. J.* 151 (2009) 30-38.
- [41] S. Sankaraiah, J.M. Lee, J.H. Kim and S.W. Choi, *Macromolecules* 41 (2008) 6195-6204.
- [42] X. Lu, Q. Yin, Z. Xin and Z. Zhang, *Chem. Eng. Sci.* 65 (2010) 6471-6477.
- [43] X. Song, P. Gunawan, R. Jiang and S.S. Jan Leong, K. Wang, R. Xu, *J. Hazard. Mater.* 194 (2011) 162-168.
- [44] H. Karami, M. Ghamooshi-Ramandi, S. Moeini and F. Salehi, Low temperature hydrothermal synthesis of MnO<sub>2</sub> nanoclusters as positive material of RAM batteries, *J. Clus. Sci.* 21 (2010) 21-34.
- [45] M. Villalobos, J. Bargar and G. Sposito, Mechanisms of Pb(II) Sorption on a Biogenic Manganese Oxide, *Environ. Sci. Technol.*, 39 (2005) 569-576.
- [46] Q. Su, B. Pan S. Wan, W. Zhang and L.Lv, Use of hydrous manganese dioxide as a potential sorbent for selective removal of lead, cadmium, and zinc ions from water, *J. Colloid Interface Sci.* 349 (2010) 607-612.
- [47] R. Liu, H. Liu, Z. Qiang, J. Qu, G. Li and D. Wang, Effects of calcium ions on surface characteristics and adsorptive properties of hydrous manganese dioxide, *J. Colloid and Interface Sci.* 331 (2009) 275-280.
- [48] Kh. Z. Elwakeel, G. O. El-Sayed and Ramy S. Darweesh, Fast and selective removal of silver (I) from aqueous media by modified chitosan resins, *Int. J. Min. Proc.* 120 (2013) 26-34.
- [49] L. Fan, C. Luo, Z. Lv, F. Lu and H. Qiu, Removal of Ag<sup>+</sup> from water environment using a novel magnetic thiourea-chitosan imprinted Ag<sup>+</sup>, *J. Hazard. Mater.* 194 (2011) 193-201.
- [50] A. Sari and M. Tüzen, Adsorption of silver from aqueous solution onto raw vermiculite and manganese oxide-modified vermiculite, *Micropor. Mesopor. Mater.* 170 (2013) 155-163.
- [51] J. Gong, L. Chen, G. Zeng, F. Long, J. Deng, Q. Niu and X. He, Shellac-coated iron oxide nanoparticles for removal of cadmium(II) ions from aqueous solution, *J. Environ. Sci.* 24 (2012) 1165-1173.
- [52] S. Liang, X. Guo, N. Feng and Q. Tian, Adsorption of Cu<sup>2+</sup> and Cd<sup>2+</sup> from aqueous solution by mercapto-acetic acid modified orange peel, *Coll. Surf. B* 73 (2009) 10-14.
- [53] S. Wan, M. Ma, L. Lv, L. Qian, S. Xu, Y. Xue and Z. Ma, Selective capture of thallium(I) ion from aqueous solutions by amorphous hydrous manganese dioxide, *Chem. Eng. J.* 239 (2014) 200-206.
- [54] M. Xu, H. Wang, D. Lei, D. Qu, Y. Zhai and Y. Wang, Removal of Pb(II) from aqueous solution by hydrous manganese dioxide: Adsorption behavior and mechanism, 25 (2013) 479-486.
- [55] B. Pan, W. Du, W. Zhang, X. Zhang, Q. Zhang, B. Pan, L. Lv, Q. Zhang and J. Chen, Improved adsorption of 4-nitrophenol onto a novel hyper-cross-linked polymer, *Environ. Sci. Technol.* 41 (2007) 5057-5062.